UCRL--94147

DE86 007116

Characterization of High Power Flashlamps and Application to Nd:Glass Laser Pumping

H. T. Powell
A. C. Erlandson
K. S. Jancaitis

This paper was prepared for submittal to
O-E/Lase '86 Conference
Los Angeles, CA
January 19-24, 1986

January 17, 1986

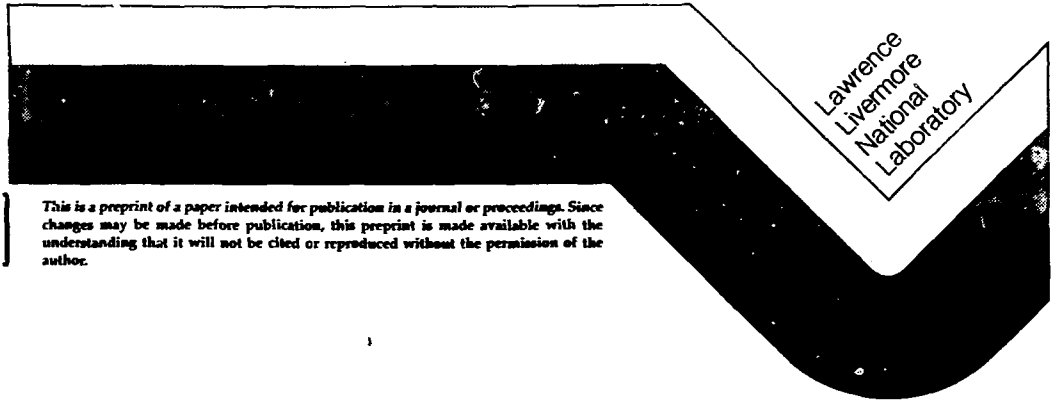

Characterization of High Power Flashlamps and Application to Nd:Glass Laser Pumping

H. T. Powell, A. C. Erlandson, and K. S. Jancaitis*

Lawrence Livermore National Laboratory

University of California

P.O. Box 5508, L-490

Livermore, California 94550

Abstract

Detailed spectral and temporal measurements of the output radiation from Xe flashlamps are reported together with their use in predicting the pumping efficiency of Nd-doped laser glass. We have made absolute spectral-intensity measurements for 0.5, 1.5, and 4.2-cm-bore flashlamps for input powers ranging from 5 to 90 kW/cm^2 and pulselengths of 600 μs. Under quasi-stationary conditions these flashlamps emit essentially identical spectra when excited at equal input power per unit-area of the bore. This behavior is characteristic of an optically-thick radiator although it is not completely clear why flashlamps should behave this way. A simple model is also described which accounts for the transient response of flashlamps by characterizing the output spectra and radiation efficiencies in terms of the radiant output power rather than the electrical input power.

*Work performed under the auspices of the U.S. Department of Energy by Lawrence Livermore National Laboratory under Contract No. W-7405-ENG-48.

Introduction

Pulsed rare-gas arc lamps are familiar modern devices with applications ranging from simple flash photography to optical pump sources for solid-state lasers. Because flashlamps provide extremely intense and short light-pulses (by pre-laser standards), Edgerton developed and applied flashlamps to stop-action photography in the 1940's and 1950's with remarkable results.[1] In 1960, Maiman used these same properties to demonstrate the first visible laser, flashlamp-pumped ruby.[2] Today at our Laboratory, flashlamps are being used in thermonuclear fusion research to pump the Nd:glass laser medium of the Nova laser.[3] The Nova system contains more than 6000 flashlamps which are excited by a capacitor bank of approximately 60 MJ. This device has produced a few-nanosecond, 1-μm-wavelength laser pulse having an energy greater than 100 kJ.

Despite the widespread application of flashlamps, there is relatively little information in the Western scientific literature specifically describing models of flashlamp plasmas or even detailing absolute spectral measurements of their optical output. By contrast there is a large body of work on pulsed lamps which has been done in the Soviet Union in the past several decades as summarized in the recently-translated book, "Pulsed Light Sources" by I. S. Marshak.[4] The lack of scientific interest in the West is likely motivated by the fact that our commercially-developed lamps indeed work well and are simple to use. Moreover, the arc physics involved in pulsed lamps, when looked at in detail, is an extremely complex subject. However, to improve the

performance of flashlamp-pumped solid-state lasers and to build fusion drivers which are even larger than Nova, it is necessary to obtain a much more detailed knowledge of flashlamps.

There are several areas which need to be studied thoroughly before flashlamp pumping of solid-state lasers can be understood in detail and reduced to a predictive science. These include:

- the electrical characteristics of flashlamps
- the absolute, time-dependent emission intensities in various spectral regions
- the cavity transfer efficiency of light from the lamps to the laser material
- the absorption of emitted radiation by the flashlamp itself
- and finally, the conversion efficiency by the flashlamp of this absorbed optical power to further emission.

The first three factors are obvious while the last two require a brief explanation. Because flashlamps are quasi-blackbody emitters, they can absorb as well as emit light. As shown in the following paper,[5] this absorption of pump radiation by the flashlamps themselves is extremely important in affecting laser performance. Furthermore, there is the question of what happens to this absorbed optical power. Is it exactly equivalent to an equal increment of electrical power or does it affect the lamp in some more complicated manner? In this and the following paper we will address, at least briefly, all but the last question.[6]

In the work reported here, we have studied the optical performance of Xe flashlamps over a broad range of bore diameters, from 0.5 to 4.2 cm. A primary interest has been to determine whether very large flashlamps

(greater than 2-cm bore) are feasible for use in fusion lasers. We have made absolute radiant output measurements in each case and have determined the instantaneous spectral distributions at peak emission for a wide range of input powers. From these studies we have discovered that the output spectral distributions of flashlamps operating in the quasi-stationary regime (for pulselengths longer than 100 μs and after arc expansion is complete) are extremely well characterized by the electrical input power per unit-wall-area of the bore as opposed to the input power per unit-volume or the electrical current density. This behavior is characteristic of an optically-thick radiator although it is not readily apparent that flashlamps should behave in this manner. We have used the measured spectral intensities to predict the instantaneous pumping efficiency of Nd:glass and have constructed a laser-pumping model which includes a rudimentary model of the flashlamp's transient response. Our transient description includes a treatment of the energy required to establish the arc and the time delay between input and output power, and it characterizes the emission spectrum by the instantaneous lamp output. Some of the results presented here are described more thoroughly in the sections of the 1982, 1983, and 1984 Laser Program Annual Reports[7] which discuss laser research and development.

General Aspects of Flashlamp Physics

The light-emitting arcs in pulsed rare gas flashlamps are generally assumed to be in local thermodynamic equilibrium (LTE). This means that at a given position and time the neutral atoms, ions, and electrons are

all described by a single temperature T which characterizes their kinetic energies and excited state populations. LTE occurs at sufficiently high electron densities where the communication of populations is primarily controlled by collisions in the plasma as opposed to wall collisions or spontaneous radiation. For a Xe flashlamp operating at typical conditions the temperature is of order 10,000°K and the electron density is of order 10^{17} cm^{-3}. Although the LTE approximation is generally believed to be good for flashlamps, there are certainly times when it is not valid (for example, during the arc-expansion phase where the electron density is relatively small).

Although the particles in a flashlamp plasma may be in equilibrium at a well defined temperature, the radiation generally is not. Kirchoff's Law states that if the absorption coefficient at wavelength λ is given by $\alpha(\lambda)$, then the emission intensity as viewed through a uniform plasma at temperature T and over a length x is given by[8]

$$I(\lambda,T) = [1 - e^{-\alpha(\lambda)x}] I_{BB}(\lambda,T) \qquad (1)$$

where $I_{BB}(\lambda,T)$ is the blackbody intensity at the temperature T. The factor in brackets is defined as the emissivity at the wavelength λ. Note that the emissivity exactly equals the absorption that a photon would suffer over the same path length. LTE plasmas can still have considerable structure in their output spectra because of the wavelength dependence of their emissivity. However, as the plasma becomes black ($\alpha x \gg 1$) these features wash out and the output saturates at the blackbody intensity. Qualitatively, this describes how flashlamps behave as their input power is increased.

These thermodynamic considerations however, do not address the physical processes which actually cause flashlamp emission. As described more fully in Marshak,[4] flashlamp light has two primary sources: bound-bound emission producing the familiar spectral lines of the gas and free-bound emission producing a continuum spectrum. Free-free electron radiation only becomes appreciable at wavelengths longer than 1 μm. The free-bound emission process is an event in which an electron collides with an ion and recombines to form an excited neutral atom by emitting a photon. This is a very improbable process which becomes significant only at high plasma densities. (At an electron density of 10^{17} cm^{-3} the time scale for electrons to radiate by this process is of order 10 μs). Nonetheless, for most flashlamp conditions of interest for pulsed laser-pumping, free-bound emission is the dominant process by which the plasma loses energy.

The intensity of free-bound emission (and absorption) generally decreases as the photon energy is increased. This occurs because both the density of electron-ion pairs and the probability of their radiative recombination decrease at higher energies. Hence, as the input power to a flashlamp is increased (increasing the electron density), the flashlamp output tends to saturate at its blackbody intensity first at long wavelengths and then at progressively shorter and shorter wavelengths. Nonetheless, we find that Xe flashlamps never get to a true blackbody output over the entire visible region at any reasonable loading. The change in emissivity with loading, together with a slight increase in temperature, causes the flashlamp output to blue-shift as the input power is increased.

The simplest radiative model of a flashlamp is a uniform cylinder of hot plasma which fills or nearly fills the lamp bore and is described by a temperature and a spectrally-dependent absorption coefficient. Trenholme and Emmett formulated an empirical model[9,10] of the flashlamp output on this basis giving specific functions, derived from experiments, for the temperature and absorption coefficient (emissivity) as a function of current density and lamp diameter. In the present studies, we have provided the data to refine this model based on a broader range of experimental results and we have developed a simple description of the transient flashlamp response.

Although this simple gray-body model may be adequate to describe the optical properties of a flashlamp from an empirical point of view, the plasma physics of a flashlamp is much more complicated as illustrated by Fig. 1. Since the arc never completely fills the lamp bore, there is always a region of cold and dense gas which surrounds the hot and lower density core. When the lamp is fired, a substantial fraction of the initial gas fill can be "squeezed" into this cold region;[11] moreover, some gas can be pushed beyond the lamp electrodes. Hence a sizeable impediment to plasma modeling of flashlamps is the lack of knowledge of the neutral-atom density in the arc. Without this information, one cannot accurately calculate the electron density, the electrical impedance, or other parameters of importance even though the temperature may be known from optical measurements.

The framing-camera picture also shown in Fig. 1 supports this view. The arc was initiated along the wall with a straight, grounded trigger-wire running along the outside of the lamp at the bottom of the

photo. Taken at the peak of the light output, the photograph shows that the arc did not fill the bore, was offset toward the initiation side, and had ragged boundaries. The dark line across the center of the picture is an artifact of the framing camera. Completely different pictures can be obtained by varying the trigger-wire geometry. For example, with a spiral trigger wire the arc follows the wire unless the spiral is wound so tightly that the arc effectively "jumps" from turn to turn. Given these complexities, it is surprising that there are good empirical laws describing the electrical impedance of a lamp and its optical output which are valid over a large range of conditions and which depend simply on the bore diameter and the total input power.

Electrical Characteristics of Flashlamps

A remarkably accurate, empirical description of the voltage-current relationship of Xe flashlamps in steady state was discovered by Gonez:[12]

$$V = K_o I^{1/2} = k_o \left(\frac{\ell}{d}\right) I^{1/2} \quad . \tag{2}$$

The lamp arc length is given by ℓ and the bore diameter by d. The dependence on ℓ and d in Eq. 2 gives a microscopic relationship between current density and electric field which is independent of bore diameter and arc length. The impedance parameter K_o depends slightly on fill pressure according to the relation[13]

$$k_o = 1.3 \left(\frac{p}{450}\right)^{0.2} \quad (V/A^{1/2}) \tag{3}$$

where p is the initial fill pressure in Torr. This same law with slight variations in the constants applies for Ar and Kr-filled lamps.

An example of the current, voltage, and impedance parameter curves for the flashlamps used in the Nova laser are shown in Fig. 2. Typical Nova flashlamps have a bore diameter of 1.5 cm, an outside diameter of 2 cm, an arc length of 112 cm, and a fill pressure of 300 Torr of Xe. Another type of flashlamp used in Nova has a bore diameter of 1.9 cm and an arc length of 47 cm. The Nova lamps are constructed of cerium-doped quartz which absorbs most of the ultraviolet radiation emitted below 0.37 μm. Two such 112-cm lamps are typically excited in series by a L-C circuit charged to about 20 kV. We used C = 87 μF, L = 480 μH, and V_b = 22 kV in this example. The time constant of our circuit

$$T = \sqrt{LC} \tag{4}$$

was 205 μs. For reasons discussed below, we refer to this as a 615-μs (3T) pulselength.

This figure shows that the voltage drops rapidly as the lamp breaks down and then is well described by the Goncz relation over most of the pulse (K_o = 90 V/A$^{1/2}$ from Eqs. (2) and (3)). The slight oscillations apparent in the voltage curve are caused by gas acoustics[14] which are sensitive to the triggering configuration, lamp diameter, and gas fill pressure. We have found the Goncz relationship applies nearly as well for flashlamps of similar length with bore diameters ranging from 0.5 to 4.2 cm. This is remarkable given that the arc expands in time (up to peak input) and that the degree of bore-filling varies with lamp diameter.

Despite its lack of a fundamental basis, the empirical Goncz relation is extremely valuable in designing electrical drive circuits for flashlamps. We typically want the excitation pulse to be critically-damped as opposed to overdamped (slowly decaying) or underdamped (ringing). Since the effective resistance of a flashlamp varies with current ($R_{eff} \sim I^{-1/2}$), the criterion for "critical damping" is somewhat different than for a simple L-C-R circuit. Emmett and Markiewicz[15] found that the appropriate damping parameter for a flashlamp in a L-C circuit is given by

$$\alpha = \frac{K_o}{\sqrt{V_b Z_o}} \tag{5}$$

where V_b is the bank charge voltage and Z_o is the bank impedance parameter $\sqrt{L/C}$. They found that for an α of approximately 0.8, the circuit is critically-damped. For larger values of α, it is overdamped and for smaller values it is underdamped. The circuit used in Fig. 2 has a calculated α of 0.8.

Because the value of α varies with charge voltage, flashlamps have the annoying property that their electrical pulseshape varies with input energy if one varies only the bank voltage V_b. This is troublesome in our work since we would like to determine the relative effectiveness of different lamps in exciting Nd:glass over a broad range in energy loadings. Since the Nd* decay time is typically comparable to the lamp output pulselengths, the peak energy storage level depends on pulsewidth and hence α. We dealt with this problem by adjusting the circuit for different flashlamps to give the same α at an input energy corresponding to the same fraction of the explosion energy.

The explosion energy of a quartz-envelope, Xe flashlamp is usually defined as[16]

$$E_x = 20{,}000\ \ell d\ (LC)^{1/4} \qquad (6)$$

where ℓ and d are given in cm, L and C are given in Henries and Farads, and E_x is in Joules. Once again this is an empirical relationship which is true for relatively long pulses ($3T > 100\ \mu s$), giving the input energy for which a flashlamp is expected to explode on a single shot. Unlike the Goncz I-V relation, this law has a simple physical explanation. The explosion energy is proportional to the inside area of the lamp bore ($\pi\ell d$) and is proportional to the square root of pulselength ($T^{1/2}$). Those familiar with thermal diffusion should recognize that the explosion energy is related to the peak temperature on the inside of the quartz wall as limited by thermal diffusion into the quartz (assuming that some fixed fraction of the electrical input power is deposited on the inside surface). Lamp explosion is apparently governed by melting of the quartz wall as opposed to other effects such as mechanical failure caused by overpressure (Notice in Eq. (5) that mechanically-related factors such as wall thickness and gas fill pressure do not appear). When the inside surface of the quartz melts, most of the electrical input gets directed into the wall causing the lamp to explode. Supporting this view, we have observed that above an explosion fraction of 0.5, appreciable white powder (devitrified quartz) appears on the inside wall of the lamp indicating that melting and vaporization has occurred.

It is convenient to define the term explosion fraction (f_x) which is the ratio of input energy to the explosion energy defined by Eq. (6). At constant pulselength, f_x is a measure of the input energy per unit-wall-area. An explosion fraction of 0.2 is a relatively safe operating point and gives long flashlamp lifetimes (~ 10^6 shots) for well-constructed lamps. The value of f_x for the conditions of Fig. 2 is 0.18, which is typical of where our flashlamps are run in fusion amplifiers. For most purposes, flashlamp operating points above an f_x of 0.3 are unsafe and impractical. However, it is important to remember the physics behind Eq. (5). If for some reason the arc does not fill the bore (perhaps because of large bore diameter and/or high fill pressure) or the lamp does not radiate efficiently, a flashlamp can explode at much lower input energies. Our definition of f_x according to Eq. (5) is, however, irrespective of what energy the flashlamp will actually explode.

We experimentally compared flashlamps of different diameter, attempting to maintain the same pulseshape at the same explosion fraction. From Eqs. (4), (5) and (6) together with the relation $E_b = 1/2\ CV_b^2$, one can easily determine how C, L, and V_b scale with lamp diameter to give a fixed variation of α with f_x. Keeping the explicit dependence of K_o on d, ℓ and k_o, one finds

$$C \sim \frac{d^{5/3}}{\ell\, k_o^{4/3}}\,, \qquad L \sim \frac{1}{C}\,, \qquad V_b \sim \frac{k_o^{2/3}\,\ell}{d^{1/3}}\,. \tag{7}$$

In a similar fashion one can determine how C, L, and V_b vary with pulselength (T) to get the same α at the same f_x.[5]

Starting with the conditions defined for the 1.5-cm-bore lamps in Fig. 2, we determined equivalent circuit parameters for flashlamps of 0.5 and 4.2-cm bore diameter. Experiments using these predicted circuit parameters showed that this scaling works reasonably well. We have found that a sensitive test for comparing pulseshapes at constant T is to compare the 10% - 10% width ($\tau_{0.1}$) of the input power pulse versus explosion fraction. This width varied from 800 to 600 μs over the range of explosion fractions studied. For reference, the width $\tau_{0.1}$ is given within a few percent by 3T at $\alpha = 0.8$. Following previous convention, we refer to 3T as the input pulselength.

Experimental Set-up

The circuit that we used in flashlamp testing is schematically shown in Fig. 3. The switch S is a size "D" ignitron capable of handling very large currents. The lumped inductance L includes the disributed circuit inductance (32 μH in our case) as well as a physical inductor. The resistance R represents an unavoidable resistive loss which we measured to be 0.28 Ω. A preionization pulse was provided by the capacitor C_p, charged to the voltage V_p and switched by S_p to break down the lamp slightly before S was fired. Such preionization allowed the use of smaller bank voltages and hence smaller input energies. We have also found that preionization increases the radiant efficiency of flashlamps, particularly for short pulses.[5] A preionization circuit similar to this is used in Nova to provide a preionization lamp check (PILC) but is not designed to be fired simultaneously with the main bank. The switch

S_p was a size "A" ignitron and C_p was approximately 1% of the bank capacitance. The preionization charge voltage V_p was negative while V_b was positive so that both delivered a negative high-voltage pulse to the lamp. One can easily show that when S_p is closed (with S open) a negative pulse which the sum of V_p and V_b is delivered to the lamp from a capacitance which is the series sum of C and C_p (approximately C_p). The preionization circuit was typically fired 200 μs before the main switch and V_p was chosen to give the sum of V_b and V_p equal to 15 kV. When preionization was needed at higher bank voltages, C_p was left uncharged and S_p was closed to preionize the lamp. The practical operating range of V_b was from 6 to 28 kV.

A schematic diagram of the experimental setup used in our optical measurements is shown in Fig. 4. All the lamps studied had an arc length of 112 cm. The 0.5 and 1.5-cm-bore flashlamps were constructed commercially (ILC) with glass to metal seals while the 4.2-cm lamp was fabricated at our laboratory and used O-ring seals. All the lamps were constructed of clear-fused-quartz, used sintered-tungsten electrodes, and had a fitting to allow the gas fill to be changed. In some cases an identical ballast lamp, placed in a black box, was connected in series to double the required bank voltage (see Eq. 7). The current was returned in a symmetric fashion to minimize magnetic forces on the lamps, allowing very large currents to be used. The flashlamps studied were mounted on a common centerline with a fixed distance of the lamp axis from the scatter plate of 23 cm. The purpose of the scatter plate was to "angle-average" the flashlamp emission as we will discuss below. The optical diagnostics were carefully apertured to view only the scatter plate and to block observation of any direct lamp emission or stray reflections.

One can see from Eq. (1) that the spectrum observed from a flashlamp can vary with the angle of view since the optical path length x becomes larger as the viewing angle is increased (as measured from the lamp normal). This effect is significant as shown in Fig. 5. The peak 1-μm fluorescence signal observed from a small sample of Nd:glass (a peak Nd-fluorescence detector) divided by the input energy to the lamp is plotted versus the input energy to the lamp for various angles of view. These data were taken by placing the lamp on a turntable and aperturing the detector so that the it observed a fixed lamp length at all viewing angles. Since the Nd:glass is pumped only over the spectral region from 0.4 to 1.0 μm, the falloff in this curve is a measure of the blue-shift of the flashlamp output with loading. Clearly, the curves have different shapes. Notice that the rollover in the curves occurs at lower input energies at larger viewing angles implying a greater blue-shift as we expect.

For the purposes of determining laser pumping, we need to know the angle-averaged emission spectrum. An angle-averaged light sample was provided by a small scatter plate located at the center of the lamp, as shown in Fig. 4. The Lambertian scatterer provides angle-averaging by scattering light which emanates from different positions along the lamp length and hence different emission angles with respect to the normal. It is easy to show that this setup provides averaging out to a maximum angle defined by the position of the scatter plate relative to the ends of the lamp (68° in our case). Because the flashlamp emission falls off with emission angle approximately as $\cos\theta$, this arrangement provides a very good angle-average.

For the scattering surface, we used pressed $BaSO_4$ powder (Eastman White Reflectance Standard) which provides a Lambertian scattering surface whose reflectivity is nearly independent of wavelength over the full emission range of our clear-fused-quartz flashlamps (0.2 to 3 μm).[17] Integrating-sphere paint, $BaSO_4$ in an organic binder (Kodak 6080), is inappropriate for this use because its reflectivity degrades in the UV after exposure to intense flashlamp light.

We have also found that integrating spheres are not suitable for angle-averaging of flashlamp emission. First, the problem of the reflectance loss in the UV of the white paint is compounded by multiple reflections. More fundamentally, with the flashlamp under study mounted inside the integrating sphere, a varying amount of flashlamp light is absorbed by the lamp, depending on wavelength and lamp loading. This distorts the measured spectrum and tends to push the results toward a blackbody distribution, at least at wavelengths where the sphere reflectivity is high.

We used several electrical and optical diagnostics to monitor lamp performance. The differential voltage across the lamp was measured as a function of time with two high-voltage probes (Tektronix 6015) and the current through the lamps was measured with a Rogowski-type coil (Pearson 1703 or 1423). Three optical diagnostics viewed the light reflected by the scatter plate: a peak Nd-fluorescence detector (PFD), a filtered or unfiltered pyroelectric detector (Molectron P1-35), and a time-gated spectrum analyzer (Tektronix J-20). The time dependent signals were digitized at 2-μs intervals (Tektronix 5223 oscilloscopes) and all signals were fed into a computer (Digital LSI 11/23) for numerical processing.

The peak fluorescence detector consisted of a silicon photodiode and a 10-nm-wide bandpass filter centered at 1.06 μm attached to the side of a small sample of Nd-doped laser glass (Owens-Illinois ED-3, 1.3-cm thick). The PFD provided a relative measure of the Nd:glass pumping efficiency of a given lamp configuration. To take out the nearly-linear variation of peak signal with input energy, we usually plotted the peak Nd* signal divided by the input energy to the flashlamp.

The pyroelectric detector, a thermally-sensitive device, had a flat spectral response over the full range of flashlamp emission wavelengths. The device was commercially provided with an operational amplifier whose feedback resistor (1 MΩ) we chose to give a 2-μs time-response and a sensitivity of about 1 V/W. We used this detector either unfiltered to determine the relative output power versus time or with a color filter to isolate various regions of the spectrum. By comparing the unfiltered pyroelectric detector signal to the signal with a 0.4-μm long-pass filter (Hoya L-42) and with a 1.0-μm long-pass filter (Corning 7-56), we were able to determine the fraction of the flashlamp output at wavelengths below 0.4 μm, at wavelengths from 0.4 to 1.0 μm, and at wavelengths longer than 1.0 μm. This required knowledge of the average transmission of the specific flashlamp spectrum for each filter over its passband. We obtained this information by convolving the wavelength-dependent filter transmissions with the spectrum measured using the spectrum analyzer from 0.4 to 1.0 μm together with a simple blackbody extension at longer wavelengths.

The Tektronix J-20 spectrum analyzer utilizes a silicon Vidicon detector. Our decision to use the J-20 was based primarily on the width of its spectral response, nominally 0.35 to 1.1 μm, and on the convenience of interfacing it to our computer. The J-20 is, in essence, a 512-element detector which is attached to the output plane of a 0.25-m spectrometer. By using color filters to eliminate second-order light and by piecing together results from three separate shots taken over three different spectral ranges, we were able to obtain time-resolved spectra from 0.4 to 1.0 μm with about a 1-nm spectral resolution. However, such spectra were obtained only after overcoming several formidable obstacles posed by the J-20.

The first problem was that the J-20, like all non-intensified silicon Vidicons, has no fast-gating capability. Our device was typically set to integrate light for 50 ms between readouts. We obtained time-resolved spectra by using a fast rotating wheel (8000 rpm) with a 1-mm-wide slit to provide a mechanical gating of light into the entrance slit of the spectrometer with a FWHM of 25 μs. The firing of the bank was electronically controlled to place the shutter opening, typically at the peak of flashlamp output, with a precision of 10 μs. A second major problem was that the output of the silicon Vidicon detector is not linear with light input when used with pulsed sources. This problem is caused by the phenomenon known as lag, which is strictly an electronic effect.[18] We corrected for this nonlinearity in software by converting from signals to intensities using an experimentally determined calibration function. This function was obtained by comparing spectral signals from a pulsed tungsten lamp (shuttered electronically with a

controllable opening time longer than 1 ms) to those obtained from the same source optically attenuated by a factor of two. He then used a 1-kW, pulse-shuttered tungsten source as an optical calibration standard (Optronics S559) to determine the response of the instrument as a function of wavelength. Flashlamp spectra were obtained by first converting the measured signals to intensities, and then correcting for the spectral response of the instrument.

Rather than relying on the absolute calibration of our optical instruments, we chose to base our absolute spectral intensity measurements on calorimetry. Our calorimeter consisted of a 15-cm-diam, black-anodized copper can which surrounded the flashlamp and had end plates to "close" the can at the lamp electrodes. Nine thermocouples were placed at equal-mass intervals along the can to produce a spatially-averaged temperature measurement. When the lamp was fired, the thermocouple signal rose in a few seconds and then decayed over several minutes. The optical energy deposited in the can was determined from the measured temperature rise and the known heat capacity of copper. Notice that the black-can technique measures only fast-pulsed radiation since heat deposited in the flashlamp envelope and elsewhere causes only a small temperature rise and radiates very slowly to the can.

Given the radiant output energy as measured by the black can, the pyroelectric detector provided the output power of the flashlamp versus time. To check the self-consistency of these measurements, we compared the time-integral of the unfiltered pyroelectric detector with the energies measured from the black can for a 1.5-cm-bore flashlamp at a variety of input energies and with Ar, Kr, and Xe gas fills. The two

signals were proportional within our errors for all conditions investigated. Using this "calibration" of the pyroelectric detector, we often used the pyroelectric detector signals to determine output energies and powers without calorimetric data.

Time-Integrated Measurements

Figure 6 shows the radiant efficiencies that we obtained with a 1.5-cm-bore, clear-fused-quartz flashlamp excited by a 635-μs pulselength and filled with either Xe (300 Torr), Kr (550 Torr), or Ar (750 Torr) as a function of explosion fraction. The radiant efficiency is defined as the radiant output energy divided by the electrical input energy. These data were obtained from can calorimetry and were taken without lamp preionization. With preionization, the efficiency values are slightly higher as shown for Xe in Fig. 7. The fill pressures for Kr and Ar were chosen to give similar electrical impedance to Xe and were within broad regions of fill pressure where the optical performance does not vary significantly.

One should note from Fig. 6 that the radiant efficiencies are all remarkably high. Xenon produces the best performance but is closely followed by Kr and Ar.[19,20] The falloff in efficiency at low inputs is likely caused by the greater importance at low inputs of the energy investment necessary to establish the arc. The slight falloff at high inputs is probably the result of an increase in UV radiation which is not transmitted through the quartz wall. In fact, given the limited passband

of the quartz, it is interesting to speculate how much of the inefficiency seen throughout is caused merely by optical absorption in the lamp wall.

Figure 7 compares the radiant efficiencies versus explosion fraction of 0.5, 1.5 and 4.2-cm-bore flashlamps, as measured from the ime-integrated pyroelectric detector signals. Again, the pulselengths were approximately 600 μs. We chose the Xe fill-pressures for optimum performance to be 750, 300 and 100 Torr for the 0.5, 1.5 and 4.2-cm-bore lamps, respectively. In contrast with Fig. 6, these data were taken with preionization. The radiant efficiency calculation includes as input energy the energy which is supplied by preionization. The preionization pulse was about 50 μs in duration, started 200 μs before the main electrical pulse, and delivered an energy to the lamp of approximately 0.4 J/cm^3. We experimentally determined that this level of preionization and this timing produced optimum performance for the 1.5-cm-bore lamp although the optimum was quite broad.

These data indicate that there is little to be gained in flashlamp efficiency by varying bore diameter, at least over the 0.5 to 4.2-cm range. We interpret the general shape of these curves to be caused by the same factors discussed for Fig. 6. Notice in comparison to Fig. 6 that the radiant efficiency of the 1.5-cm-bore flashlamp rises more quickly and reaches a higher value because of preionization. This is likely caused by faster arc expansion and reduced "arc-contact" with the wall. It is also interesting that the efficiency curves for the different diameters are nearly identical when plotted versus explosion fraction, i.e., input energy per unit-wall-area. For this pulselength

the explosion energy corresponds to an input of 91 J/cm^2 for all lamp diameters. One should also appreciate that the input electrical energies and the output optical energies of the 4.2-cm-bore flashlamp were very large, up to 48 and 36 kJ, respectively.

Figure 8 further demonstrates that input energy per unit wall area provides a much better characterization of time-integrated flashlamp output than for instance, input energy per unit-volume. In this figure we have plotted the peak-Nd* fluorescence produced by the PFD divided by E_{in} versus flashlamp loading per unit-area in (a) and versus loading per unit-volume in (b). The data for the different flashlamps are plotted absolutely without relative normalization to each other.

As shown in Fig. 8(a), the PFD data for the different flashlamps track closely when plotted versus explosion fraction (input energy per unit-wall-area). In fact some of the slight differences observed may be caused by a failure to match exactly the input pulseshapes versus explosion fraction. Again, there is no strong difference between these flashlamps for the purpose of pumping Nd:glass. The curves are grossly different when plotted versus input energy per unit-volume as shown in (b). The shape of these curves reflects the efficiency of the flashlamp in producing light in the Nd:glass pump region, between 0.4 and 0.95 μm. The rise in the peak-Nd* efficiency at low inputs parallels the radiant efficiency increase with input as shown in Fig. 7. However, the falloff in the curves at high input is much more dramatic than the falloff of the radiant efficiency, reflecting the greater effect the blue-shift has for Nd:glass pumping. (In comparing Figs. 7 and 8, one

should be aware that their y-axis scales span different relative changes). Nonetheless, the observed falloff in peak Nd^*/E_{in} is much smaller than typically observed in Nd:glass amplifiers as the following paper will discuss.

Time-Resolved Measurements

To construct a model of flashlamp pumping of solid state lasers, it is necessary to obtain time-resolved output intensities and spectral distributions. The measurements that we will now discuss are all instantaneous rather than time-integrated. They were taken at the peak of the radiant output for the same, relatively-wide, 600-μs pulses (with preionization) as described for the time-integrated measurements. Such data are representative of instantaneous flashlamp performance for quasi-stationary conditions. We will later discuss the use of these quasi-stationary results to describe the transient output of pulsed Xe flashlamps.

The instantaneous radiant efficiencies of the 0.5, 1.5 and 4.2-cm lamps are shown in Fig. 9 as a function of input power per unit-wall-area. The instantaneous radiant efficiency is defined as the ratio of the peak optical output power to the electrical input power at the time of peak radiant output. It is not meaningful to measure the instantaneous efficiency at other points in the pulse as will become apparent later. As a point of comparison, a peak input power of 45 kW/cm^2 corresponds to an explosion fraction of 0.2 at this pulselength.

Analagous to the time-integrated results, the instantaneous radiant efficiencies of the 1.5 and 4.2-cm lamps follow similar curves when graphed versus input power per area; the 0.5-cm lamp appears to behave somewhat differently. More recent data indicate the 0.5-cm-bore lamp was not adequately preionized for these results, probably causing this difference. With careful inspection of the curves, one can discern that the instantaneous efficiencies at the peak of the pulse are substantially higher than the time-integrated radiant efficiencies at low input energies; however, at high input energies the corresponding points are relatively close. We believe this difference is caused by the relatively-constant energy investment which is necessary to establish the arc. This causes the flashlamp to radiate somewhat less efficiently at early times during the pulse, lowering the time-integrated values significantly at low inputs.

A more detailed comparison of the outputs of the three different flashlamps is shown in Fig. 10. We have plotted the fractions as measured using the pyroelectric detector of the instantaneous output in the UV ($\lambda < 0.4$ μm), pump ($0.4 < \lambda < 1.0$ μm), and IR ($\lambda > 1.0$ μm) regions versus input power per unit-area. These curves show the blue-shift of flashlamp output which occurs with increasing power loading. The close agreement of the broad spectral distributions of the 0.5, 1.5, and 4.2 cm bore flashlamps when plotted in this manner is surprising. The curves for the different lamps would grossly disagree if they were plotted versus power per unit-volume or current density. The common dependence of the efficiencies and spectral distributions as a

function of input power per area as shown in Figs. 9 and 10 is consistent with our finding that the peak Nd^*/E_{in} curves scale with input energy per area as shown in Fig. 8(a).

Figure 11 shows a much more detailed comparison of the instantaneous spectral distributions of these flashlamps. We obtained these curves using the J-20 and normalized their areas to the spectral fractions in the 0.4 to 1.0-μm region found using the pyroelectric detector. The precise agreement between the flashlamp spectra at equal input power per area is indeed remarkable. As a point of comparison the current density at 46 kW/cm^2 was 4.3, 2.4, and 1.5 kA/cm^2 from the smallest to the largest bore diameter. Current density by itself is therefore not a useful parameter in comparing the spectral output of different flashlamps.

One can ask why it is that Xe flashlamps at quasi-stationary conditions produce spectra which scale with the input power per unit-area. We currently do not have a satisfactory explanation of this behavior. However, one should recognize that true blackbodies also behave in this manner. Since a blackbody radiates power proportional to its surface area, the temperature that it reaches (and hence its output spectrum) is a function of the input power per unit-radiating-area. It is puzzling that flashlamps should behave in an equivalent manner long before they reach true blackbody conditions.

The spectra in Fig. 11 further illustrate the blue-shift of the lamp output spectrum and the disappearance of spectral features as the input power is increased. The spectrometer resolution was adequate to resolve completely the observed emission features. The emission lines in the 0.75 to 1.0-μm region have been identified (more readily at lower

inputs) primarily as 6p-6s neutral Xe lines while the lines near 0.5 μm are 7p-6s neutral Xe lines. When prominent, the emission lines show no signs of self-reversal; however, at high inputs when a continuum is produced, the same lines can sometimes be seen as very small absorption features. These observations are consistent with the view that the temperature profile of the plasma is relatively flat with a sharp edge between the hot and cold regions. It is also interesting to observe that at an input of 20 kW/cm^2, the tops of the near-infrared Xe lines appear to be saturating to a common, presumably blackbody, curve.

Figure 12(a) shows examples of the instantaneous spectral distributions for the 1.5-cm-bore lamp plotted as absolute intensity distributions rather than as a fractional distributions. Notice that the output intensities saturate at long wavelength as the input power is increased and as the spectra become smooth. It may be surprising to some readers that these spectra show so little structure compared to other data which are available.[13,21] It is important to remember that these are instantaneous spectra; time-integrated spectra for the same conditions show substantially more line structure coming from early and late times in the pulse.

Figure 12(b) shows the emissivities that were inferred from the two lower curves in Fig. 12(a). To find the emissivity it was first necessary to determine the plasma temperature. This could be easily done using our absolute intensity measurement if we were certain that at some specific wavelength the emission had reached the blackbody limit. Rather than guessing the wavelength where this might occur, it is straightforward to define an effective temperature T_{eff} at every wavelength such that

$$I(\lambda) = I_{BB}(\lambda, T_{eff}). \qquad (8)$$

One might hope that the same T_{eff} would be found at a number of wavelengths where the plasma is black thus giving a single well-defined temperature. However, we have simply taken the plasma temperature to be the highest value of T_{eff} over the complete wavelength range. We then obtained the emissivity by dividing the measured intensity curve by the blackbody curve given by that temperature. This technique works only if there exists some spectral region which emits as a blackbody at the plasma temperature.

The temperatures inferred by this technique were 9200, 10,000, and 11,260°K, respectively for the 20, 41, and 67 kW/cm^2 data shown here. For lamp loadings of 40 kW/cm^2 or less, the highest T_{eff} was found near the intense 0.828-μm Xe line. Notice that the emissivities generally falloff toward shorter wavelength as previously discussed. However, also notice that the emissivities are somewhat less than one near 1 μm. This may be a "line reversal" effect where a somewhat colder region on the edge of the plasma becomes sufficiently opaque to limit the apparent temperature. This becomes more pronounced at even higher lamp loadings where we find the wavelength for the maximum T_{eff} shifts down to as low as 0.7 μm. To the degree that such effects are important, a single-temperature model is inadequate to describe the emission properties of a Xe flashlamp.

Recognizing that the emissivity is also just the angle-averaged absorption of the plasma (see Eq. 1), Fig. 12(b) also shows the effective absorption that a flashlamp presents in a laser cavity assuming a Lambertian distribution of input light. The plasma is quite absorptive

over most of the pump spectrum although the degree of blackness varies appreciably with loading. This change in the blackness of a flashlamp with input power greatly complicates the problem of modeling flashlamp-pumped solid-state lasers. In general, this change causes the transfer efficiency of pump light from the flashlamps to the laser material to decline with input. However, the importance of this effect depends strongly on the specific laser design.

Nd:Glass Pumping Efficiency Calculations

We have used the measured flashlamp spectra to calculate the instantaneous, single-pass, pumping efficiency of Nd:glass. The pumping efficiency η_{Nd} is defined as the instantaneous power which the flashlamp could provide to the laser inversion divided by the instantaneous electrical power into the lamp. This efficiency can be calculated from the spectral-overlap integral

$$\eta_{Nd}(P_{in}) = \int d\lambda \, (\lambda/\lambda_{laser}) \, I(\lambda,P_{in}) \, \{1 - \exp[-\sigma(\lambda)\rho w]\} \, P_{in} \qquad (9)$$

where P_{in} is the electrical power into the lamp, λ_{laser} is the operating wavelength of the laser, $\sigma(\lambda)$ is the absorption cross section of the laser ion, ρ is the ionic number density, and w is the thickness of the laser medium. The ratio of wavelengths in Eq. 9 is just the quantum defect while the quantity in brackets is the single-pass absorption of the laser medium. This calculation gives the efficiency that one could ideally obtain for a continuously operating laser assuming

that the pump power was transported from the flashlamps to the laser medium without loss and that the laser power was extracted from the medium without loss.

Figure 13 displays the absorption spectrum of Nd:glass (Schott LG-660) at the doping-thickness product ($\rho w = 1.6 \times 10^{21}$ ions/cm^2) used in the amplifier studies described in the following article.[5] The thickness w was presumed to be the normal-incidence path length through the disk (4.3 cm in our case). The Nd:glass is strongly absorbing over most of the pump region for these conditions. Notice in this graph as well as in the calculations that we have omitted the 0.35-μm pump band of Nd. We presume that pump radiation at this wavelength is completely blocked by the cerium-doped quartz envelopes of the flashlamps used in the amplifier experiments. At wavelengths longer than 0.4 μm, we assumed the output intensities from cerium-doped and clear-fused quartz envelope flashlamps to be the same.

Using the quasi-stationary spectral data from the 1.5-cm-bore flashlamp and the absorption data plotted in Fig. 13, we calculated the Nd pumping efficiency versus input power per area as shown in Fig. 14. Lamps of other bore diameters yield very similar results when plotted in this manner. The solid line is a fourth-order polynomial fit to the calculated points. Notice for this doping-thickness product that the pumping-efficiency values are quite high, of order 15%, at typical lamp loadings. The pumping efficiency would be reduced for smaller doping-thickness products. The decline of the curve with loading is caused by the blue-shift of the lamp. It is interesting to note that the curve does not roll over at low inputs as seen in the instantaneous

radiant efficiency curves shown in Fig. 9. The reason for this difference is that for small lamp inputs the quasi-stationary spectra better match the Nd:glass absorption, making up for the rollover in the radiant efficiency.

We have used the pumping-efficiency curve shown in Fig. 14 to calculate the expected gain in single-pass amplifier pumping experiments as discussed in the following article. However, to explain this calculation, one needs to understand the rudimentary model that we have developed for the transient behavior of flashlamps.

Transient Behavior of Flashlamps

The measurements discussed thus far have related to flashlamps under quasi-stationary conditions. One would expect for a very long excitation pulselength that the quasi-stationary results would apply throughout the pulse corresponding to the input power at each moment in time. This steady-state approximation was previously assumed by Trenholme and Emmett.[9] We find that the accuracy with which the quasi-stationary results describe the time dependence of the flashlamp output is strongly dependent on whether preionization is used. With adequate preionization, the steady-state description, with small modifications to be explained, is reasonably valid for electrical pulselengths longer than about 100 μs. Previous measurements[22] suggesting that the steady-state model is completely invalid were strongly affected by the absence of preionization.

The first modification that we have made to the quasi-stationary description takes into account the finite response time of the flashlamp plasma. In general, flashlamps do not respond instantaneously to changes in the input power. This is illustrated in Fig. 15 which shows the electrical input power and the optical output power (measured using the pyroelectric detector) versus time for our standard 1.5-cm-bore flashlamp excited by a 600-μs pulse. Both have been normalized to their peak values. Notice that the output pulse tracks the input pulse but with a time-lag of approximately 30 μs throughout. For input energies above an explosion fraction of 0.1 and with preionization, this 30-μs time-lag is characteristic of the flashlamp response for long input pulselengths. At smaller input energies, we observed somewhat longer delay times and slight shape changes between the input and output pulses.

The time delay between input and output shown in Fig. 15 just represents the time required for the flashlamp to lose (primarily by radiation) the stored energy which it contains. In essence, it is the radiative response time of the Xe plasma. Calculations of this response time which are in approximate agreement with these measurements have been discussed elsewhere.[23]

Because the plasma energy stored in steady state does not respond instantaneously to the power input, it is also clear that the output spectrum, which is presumably a function of the stored energy, does not respond instantaneously. This is shown in Fig. 16(a) where we have plotted the measured fractional distributions of the output in the UV, pump, and IR regions as a function of the instantaneous power into the

flashlamp. These data were taken over time on a single pulse using the filtered-pyroelectric-detector method. Time starts at the end of the curves starting at higher input power.

If the spectral response were instantaneous, the plots in Fig. 16(a) would double back on themselves and lie on top of the curves in Fig. 10. Clearly they do not. Notice, however, that if we plot the same spectral fractions as a function of the instantaneous output power, as shown in Fig. 16(b), much better overlap is obtained. Moreover, they are in very good agreement with the data in Fig. 10 when plotted in this manner. This agreement is reasonable since the output power and the spectral distributions both depend on the "state of the plasma" and hence should vary together aside from time-dependent changes such as arc expansion.

Figures 15 and 16 suggest a primitive method to handle the transient response of a flashlamp. We simply switch our description of the instantaneous efficiency and spectral distributions from being a function of P_{in} to being a function of P_{out}. Of course, for modeling purposes one must then determine the time dependence of P_{out}. Fortunately, we have found an empirical method for calculating $P_{out}(t)$ from a given $P_{in}(t)$ which makes physical sense.

From conservation of energy, one can easily show that the input and output power of a flashlamp are related by the differential equation,

$$\frac{dP_{out}}{dt} = [\eta(P_{out})\, P_{in} - P_{out}]/\tau(P_{out}). \qquad (10)$$

The response time in the denominator corresponds to the time-lag which we have discussed and $\eta(P_{out})$ is the instantaneous radiant efficiency as

shown in Fig. 9, determined at the point in time where dP_{out}/dt was zero. Notice we have assumed that the instantaneous radiant efficiency and the response time are both functions of P_{out} from the considerations previously discussed.

We have numerically solved this equation assuming a fixed response time of 30 μs and using the experimental input-power curves for the 1.5-cm lamp, and we have compared the predictions for $P_{out}(t)$ to the measured $P_{out}(t)$. For a 600-μs electrical pulselength and with input explosion fractions above 0.1, the agreement is excellent as one might expect. However, at smaller input energies, the predictions overestimate the output powers at short times. This disagreement indicates the need to account for the energy investment necessary to establish the arc. It is precisely this effect which makes the instantaneous radiant efficiencies shown in Fig. 9 somewhat higher than the time-integrated efficiencies shown in Fig. 7.

We have been able to correct empirically for this effect by modifying the efficiency term in Eq. 10 by a factor which accounts for the electrical energy, E(t), invested in the lamp up to that point in time:

$$\eta'[P_{out}, E(t)] = \{1 - A \exp[-E(t)/B]\}\, \eta(P_{out}) \qquad (11)$$

With this modification the agreement between the model and observations for long times and large input energies is still maintained, since at times where the input energy is much greater than the "saturation-energy", B, the instantaneous efficiency goes to its quasi-stationary value.

We have varied A and B to best-fit the experimental output powers (we actually fit the ratio of the predicted P_{out} to the measured P_{out}) for the full range of input energies and pulselength data which we had available for the 1.5-cm flashlamp with preionization. With A = 0.636 and B = 0.354 J/cm^2 the agreement was extremely good at all times and input energies down to excitation pulselengths as short as 100 μs. We have not yet determined how A and B vary with bore diameter and with preionization energy.

This method gives us a model of single-pass laser pumping which includes the transient response of the lamp. By replotting Fig. 14 using the data in Fig. 9, we obtained the pumping rate as a function of P_{out}. This approach assumes that small details in the time-dependent output spectra, which might vary at a given output power, are not important for predicting Nd:glass laser pumping. Notice that the concept of an instantaneous pumping efficiency with respect to P_{in} is no longer well defined in this model, although the instantaneous pumping rate is clearly determined. The results of this model agree very well with amplifier experiments as discussed in the following paper.

Summary

We have studied pulsed, rare-gas flashlamps specifically to obtain the information necessary to construct an accurate model of solid-state-laser pumping. We find that the time-integrated radiant efficiency (E_{out}/E_{in}) of flashlamps is quite large, approximately 75% for Xe-filled lamps constructed of clear-fused-quartz and excited at

conditions typical of their use in the Nova laser. The instantaneous radiant efficiency (P_{out}/P_{in}) defined at the time of peak radiant output is slightly larger, approximately 80%, for these same conditions.

By studying flashlamps of fixed arc length and varying bore diameters (0.5, 1.5, and 4.2 cm), we have shown that the instantaneous output spectra of flashlamps at quasi-stationary conditions is extremely well described by the input power per unit-area of the lamp bore over a large range of lamp bore diameters and input powers (the range 5-90 kW/cm^2 was studied). Moreover, there is no significant difference in either the radiant efficiency or the Nd:glass-pumping performance of flashlamps over this range of bore diameters at a given input power per area. These results have been applied to Nd:glass and an example of the predicted pumping efficiency versus input power to the lamp was given.

To construct a satisfactory pumping model, it is necessary to describe the output spectra as a function of time. Any accurate model must take into account the response time of the flashlamp plasma, approximately 30 μs at typical conditions. The degree to which the quasi-stationary results can be used to predict the time-dependent emission (steady-state approximation) has been investigated. At least within broad spectral bands, if the emission spectra are characterized in terms of P_{out} rather than P_{in}, the steady-state approximation works reasonably well. We discussed a differential equation which gives P_{out} (t) from $P_{in}(t)$ and which includes a method to account for the energy required to establish the emitting plasma.

Acknowledgement

The authors gratefully acknowledge the many contributions made by the late L. P. Bradley to the initial phases of this work. We also acknowledge the encouragement, support, and guidance given by J. L. Emmett and J. B. Trenholme to these studies. In addition, we are indebted to L. R. Truelsen, D. A. Masquelier, R. B. Behymer, and many others in the laser fusion program at LLNL for the high quality assistance they provided in performing these experiments.

References

1. H. E. Edgerton, Electronic Flash, Strobe, (McGraw-Hill, New York, 1970).
2. T. H. Maiman, "Stimulated Optical Radiations in Ruby", Nature 87, 493 (1960).
3. W. W. Simmons and R. O. Godwin, "Nova Laser Fusion Facility-Design, Engineering, and Assembly Overview", Nuclear Technology/Fusion 4, 8 (1983).
4. I. S. Marshak, Pulsed Light Sources, (Consultants Bureau, New York, 1984).
5. J. E. Murray, H. T. Powell, and B. W. Woods, "Optimized Flashlamp Pumping of Disk Amplifiers", SPIE Proceedings Vol. 609, Conference on Flashlamp-Pumped Laser Technology (1986).
6. Brief results on the efficiency of optical recycling are presented in: H. T. Powell, K. S. Jancaitis, J. B. Trenholme, C. E. Uhrich, and G. R. Wirtenson, "Recycling of Optical Radiation by Flashlamps", paper ThX3, Technical Digest of the Conference on Laser and Electro-optics, CLEO XXV, (Opt. Soc. of Am., 1985).
7. The Laser Program Annual Reports of Lawrence Livermore National Laboratory are available from: National Technical Information Service; U. S. Dept. of Commerce; 9285 Port Royal Road; Springfield, VA 22161.
8. H. C. Hottel and A. F. Sarofim, Radiative Transfer, (McGraw-Hill, New York, 1976), chap. 1.

9. J. B. Trenholme and J. L. Emmett, "Xenon Flashlamp Model for Performance Prediction" in Proceedings of Ninth International Conference on High Speed Photography, ed. H. G. Hyzen and W. G. Chase (Society of Motion Picture and Television Engineers, New York, 1970) p. 299.

10. A summary of the Trenholme-Emmett model and a review of flashlamp pumping of Nd:glass lasers is found in: D. C. Brown, High-Peak-Power Nd:Glass Laser Systems, (Springer-Verlag, Berlin, 1981), chap. 3.

11. Computer modeling whch graphically illustrates this effect is presented in: M. J. Kushner, "Arc Expansion in Xenon Flashlamps", J. Appl. Phys. 57, 2486 (1985).

12. J. H. Goncz, "Resistivity of Xenon Plasma", J. Appl. Phys. 36, 742 (1965).

13. L. Noble, C. Kretschmer, R. Maynard, H. Flentz, and L. Reed, Optical Pumps for Lasers, Final Report, Vol. 1 (ILC Technology, Inc., Sunnyvale, CA., 1971), ECOM-0239-F.

14. W. Lama and T. Hammond, "Arc-Acoustic Interaction in Rare Gas Flashlamps", Appl. Opt. 20, 765 (1981).

15. J. P. Markiewicz and J. L. Emmett, "Design of Flashlamp Driving Circuits", IEEE J. Quant. Electron. QE-2, 707 (1966).

16. J. H. Goncz, "New Developments in Electronic Flashtubes", ISA Transactions 5, 28 (1966).

17. F. Grum and G. W. Luckey, "Optical Sphere Paint and Working Standard of Reflectance", Appl. Opt. 7, 2289 (1968); see also F. Grum and T. E. Wightman, "Absolute Reflectance of Eastman White Reflectance Standard", Appl. Opt. 16, 2775 (1977).

18. R. W. Redington, "The Transient Response of Photoconductive Camera Tubes Employing Low-Velocity Scanning", IRE Trans. on Electron Devices ED-4, 220 (1957).

19. Absolute radiant efficiency measurements of Ar, Kr, and Xe-filled flashlamps also made using calorimetry are discussed in: V. V. Ivanov, V. G. Nikoforov, and A. G. Rozanov, "Energy Balance in Pulse Discharges in Rare Gases", Sov. J. Quant. Electron. 4, 717 (1974).

20. Instantaneous radiant efficiencies of Ar, Kr, and Xe-filled flashlamps for producing light between 0.4 and 1.1 μm are reported in: J. R. Oliver and F. S. Barnes, "A Comparison of Rare Gas Flashlamps", IEEE J. Quant. Electron. QE-5, 232 (1969).

21. J. H. Goncz and P. B. Newell, "Spectra of Pulsed and Continuous Xenon Discharges", J. Opt. Soc. Am. 56, 87 (1966).

22. J. H. Kelly, D. C. Brown, and K. Teegarden, "Time Resolved Spectroscopy of Large Bore Xe Flashlamps for Use in Large Aperture Amplifiers", Appl. Opt. 19, 3817 (1980).

23. A. E. Orel and H. T. Powell in Laser Program Annual Report 83, (Lawrence Livermore National Laboratory, Livermore, CA, 1984).

Figure Captions

1. Schematic diagram of the arc in a pulsed rare gas flashlamp and a framing camera picture at peak output of the visible emission from a 4.2-cm-bore, 100-Torr Xe flashlamp excited at an explosion fraction of 0.1.
2. Typical plots of voltage, current, and impedance parameter for a 1.5-cm bore, 112-cm arc-length flashlamp as used in the Nova laser.
3. Schematic diagram of the electrical circuit used to excite rare gas flashlamps.
4. Schematic diagram of the optical setup used in flashlamp studies to provide angle-averaging of the output emission.
5. Experimental measurements of the input-energy-normalized, peak Nd* fluorescence signals produced by a 1.5-cm-bore Xe flashlamp as a function of explosion fraction for various angles of view.
6. Measured radiant efficiencies of a 1.5-cm-bore flashlamp filled with either 300 Torr Xe, 550 Torr Kr, or 750 Torr Ar for a pulselength of 600 μs as a function of explosion fraction.
7. Measured radiant efficiencies of 0.5, 1.5, and 4.2-cm-bore flashlamps filled to Xe pressures of 750, 300, and 100 Torr, respectively, for a 600-μs input pulsewidth as a function of explosion fraction.
8. Experimental measurements of input-energy-normalized, peak Nd* fluorescence signals for 0.5, 1.5, and 4.2-cm-bore Xe flashlamps excited by a 600-μs pulse as a function of (a) explosion fraction and (b) input energy per unit-volume.

9. Measured values of the instantaneous radiant efficiencies P_{out}/P_{in} at peak output for 0.5, 1.5, and 4.2-cm-bore Xe flashlamps versus electrical power loading per unit-area.
10. Measured fraction of the instantaneous output radiation of 0.5, 1.5, and 4.2-cm-bore Xe flashlamps lying in the UV, pump and IR regions as a function of electrical power loading per unit area.
11. Measured instantaneous spectral distributions produced by (a) 0.5, (b) 1.5, and (c) 4.2-cm-bore Xe flashlamps at peak radiant output for electrical inputs corresponding approximately to f_x = 0.1 and 0.2 with a 600-μs pulselength.
12. (a) Measured absolute output spectral intensities produced by a 1.5-cm-bore Xe flashlamp at several input power loadings.
    (b) Spectrally-dependent emissivities inferred from some of the data shown in (a) using the method described in the text.
13. Absorption spectrum of Nd-doped laser glass (Schott LG-660) at a Nd doping-thickness product of 1.6×10^{21} ions/cm^2.
14. Instantaneous Nd-pumping efficiency for the Nd:glass absorption spectrum shown in Fig. 13 as a function of electrical input power calculated using the 1.5-cm-bore Xe flashlamp measurements.
15. Comparison of normalized input electrical power and output radiant power versus time measured for 1.5-cm-bore Xe flashlamp excited by a 600-μs electrical pulse.
16. Measured radiant fractions of the radiant output power from a 1.5-cm-bore Xe flashlamp in the UV, pump, and IR regions (see Fig. 10 for labeling) as a function of time plotted versus instantaneous input at an explosion of 0.18 and a pulselength of 600 μs.

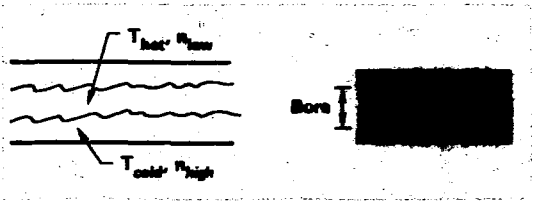
T_{hot}, n_{low}
T_{cold}, n_{high}
Bore

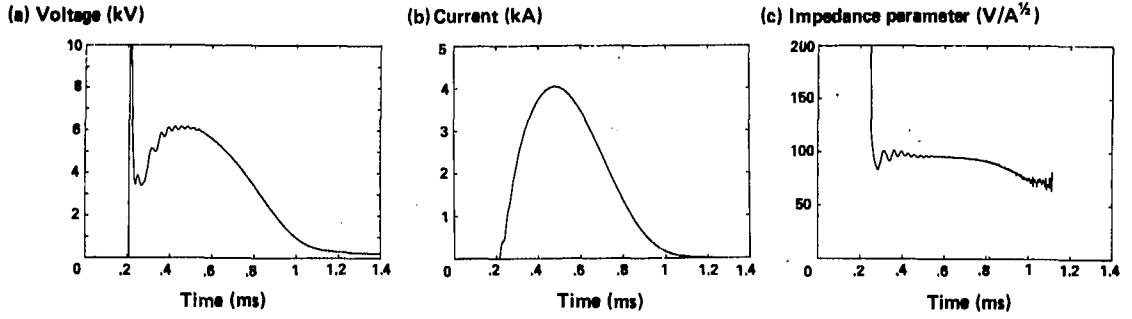
(a) Voltage (kV)
10
8
6
4
2
0
.2
.4
.6
.8
1
1.2
1.4
Time (ms)
(b) Current (kA)
5
4
3
2
1
0
.2
.4
.6
.8
1
1.2
1.4
Time (ms)
(c) Impedance parameter (V/A½)
200
150
100
50
0
.2
.4
.6
.8
1
1.2
1.4
Time (ms)

Figure 2

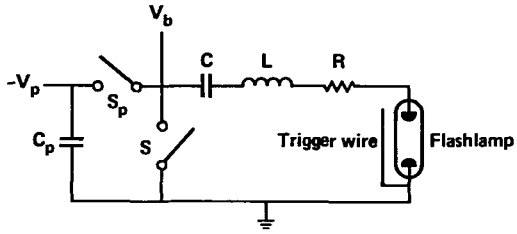

Figure 3

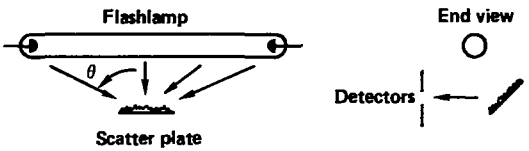

Figure 4

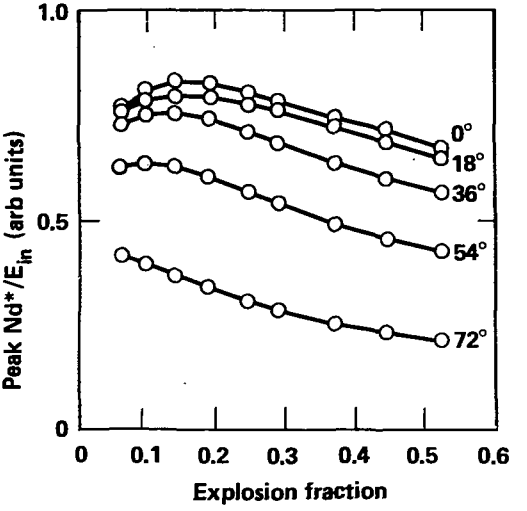
1.0
0.5
0
Peak Nd*/E$_{in}$ (arb units)
0
0.1
0.2
0.3
0.4
0.5
0.6
Explosion fraction
0°
18°
36°
54°
72°

Figure 5

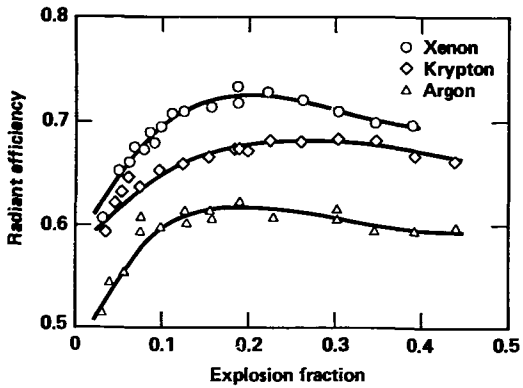
0.8
0.7
0.6
0.5
Radiant efficiency
0
0.1
0.2
0.3
0.4
0.5
Explosion fraction
Xenon
Krypton
Argon

Figure 6

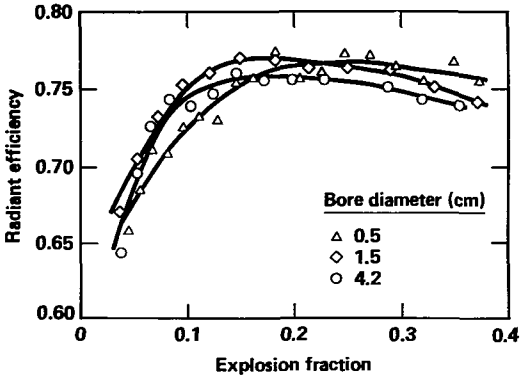
0.80
0.75
0.70
0.65
0.60
Radiant efficiency
0
0.1
0.2
0.3
0.4
Explosion fraction
Bore diameter (cm)
△ 0.5
◇ 1.5
○ 4.2

Figure 7

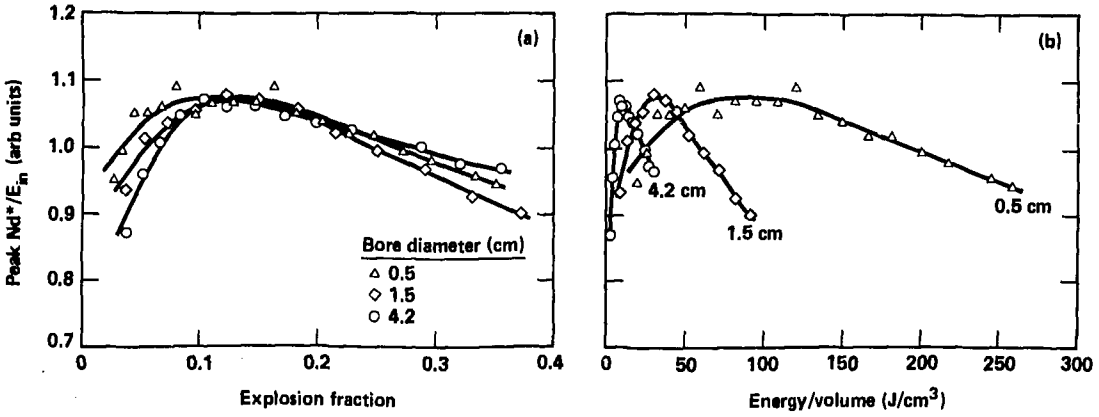
(a)
(b)
Peak Nd*/E_in (arb units)
Explosion fraction
Energy/volume (J/cm³)
Bore diameter (cm)
0.5
1.5
4.2
4.2 cm
1.5 cm
0.5 cm
1.2
1.1
1.0
0.9
0.8
0.7
0
0.1
0.2
0.3
0.4
50
100
150
200
250
300

Figure 8

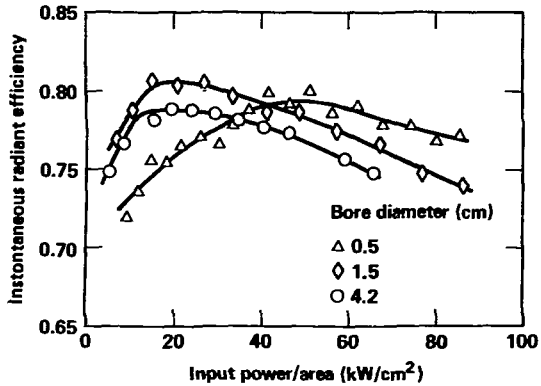
0.85
0.80
0.75
0.70
0.65
Instontaneous radiant efficiency
0
20
40
60
80
100
Input power/area (kW/cm^2)
Bore diameter (cm)
△ 0.5
◊ 1.5
○ 4.2

Figure 9

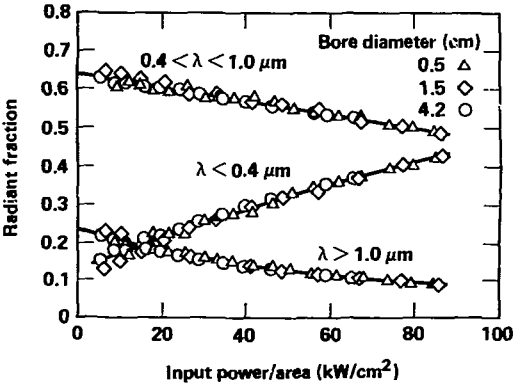
Radiant fraction
0.8
0.7
0.6
0.5
0.4
0.3
0.2
0.1
0
0
20
40
60
80
100
Input power/area (kW/cm^2)
Bore diameter (cm)
0.5 △
1.5 ◇
4.2 ○
0.4 < λ < 1.0 μm
λ < 0.4 μm
λ > 1.0 μm

Figure 10

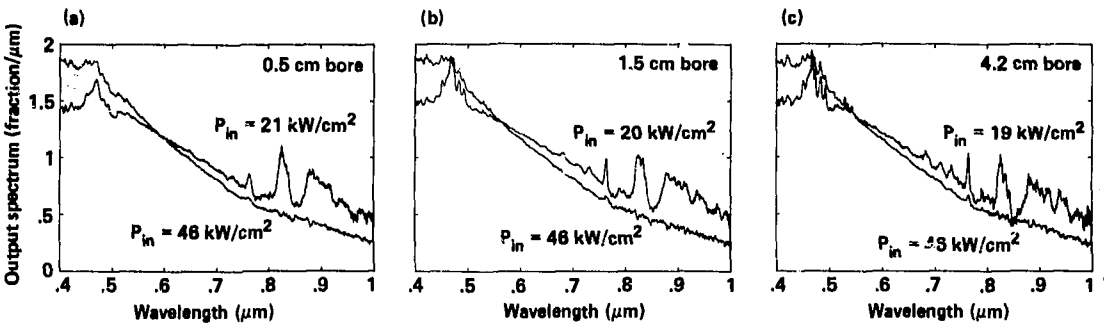
(a)
(b)
(c)
Output spectrum (fraction/μm)
2
1.5
1
.5
0
0.5 cm bore
1.5 cm bore
4.2 cm bore
P_in = 21 kW/cm²
P_in = 46 kW/cm²
P_in = 20 kW/cm²
P_in = 46 kW/cm²
P_in = 19 kW/cm²
.4 .5 .6 .7 .8 .9 1
Wavelength (μm)

Figure 11

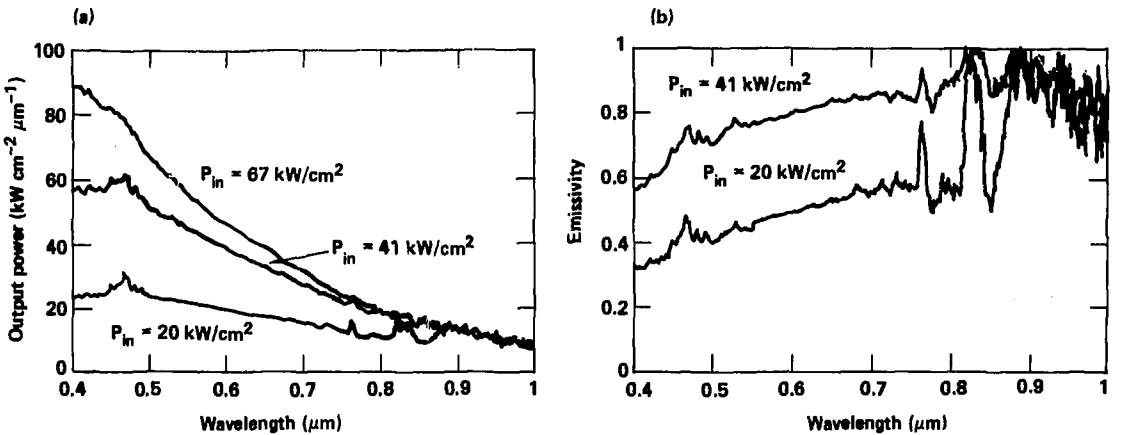
(a)
Output power (kW cm^{-2} μm^{-1})
100
80
60
40
20
0
P_{in} = 67 kW/cm^2
P_{in} = 41 kW/cm^2
P_{in} = 20 kW/cm^2
0.4
0.5
0.6
0.7
0.8
0.9
1
Wavelength (μm)
(b)
Emissivity
1
0.8
0.6
0.4
0.2
0
P_{in} = 41 kW/cm^2
P_{in} = 20 kW/cm^2
0.4
0.5
0.6
0.7
0.8
0.9
1
Wavelength (μm)

Figure 12

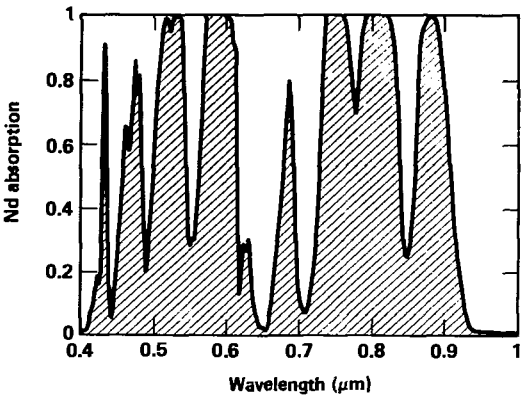

Figure 13

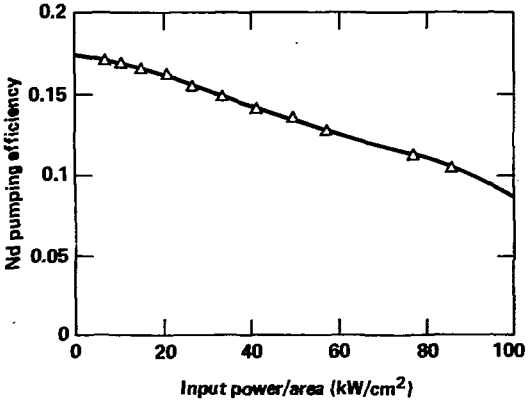
0.2
0.15
0.1
0.05
0
Nd pumping efficiency
0
20
40
60
80
100
Input power/area (kW/cm2)

Figure 14

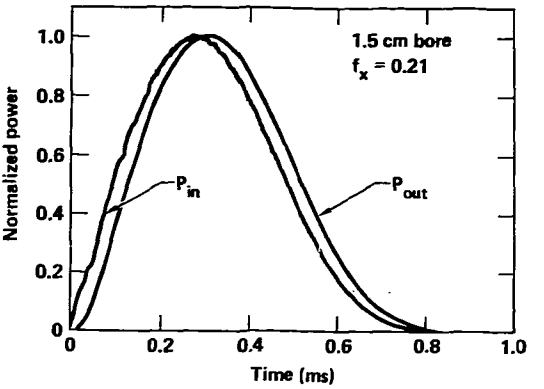
1.5 cm bore
f_x = 0.21
P_{in}
P_{out}
Normalized power
Time (ms)
0
0.2
0.4
0.6
0.8
1.0

Figure 15

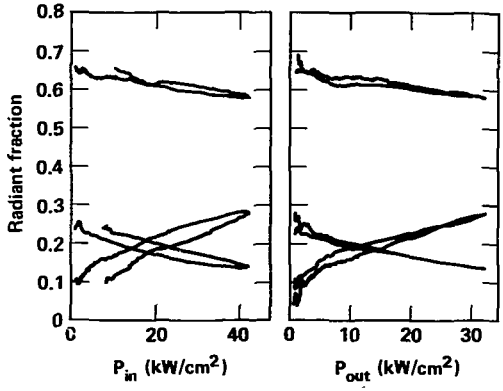
Radiant fraction
0.8
0.7
0.6
0.5
0.4
0.3
0.2
0.1
0
0
20
40
P_{in} (kW/cm^2)
0
10
20
30
P_{out} (kW/cm^2)

Figure 16